Separation Science and Technology
Publication details, including instructions for authors and subscription information:
http://www.informaworld.com/smpp/title~content=t713708471

A Theoretical Model for the Separation of Glucose and Fructose Mixtures by Using a Semicontinuous Chromatographic Refiner

Kwang Nam Lee[a]; Won Kook Lee[a]
[a] DEPARTMENT OF CHEMICAL ENGINEERING, KOREA ADVANCE INSTITUTE OF SCIENCE AND TECHNOLOGY, SEOUL, SOUTH KOREA

To cite this Article Lee, Kwang Nam and Lee, Won Kook(1992) 'A Theoretical Model for the Separation of Glucose and Fructose Mixtures by Using a Semicontinuous Chromatographic Refiner', Separation Science and Technology, 27: 3, 295 — 311

To link to this Article: DOI: 10.1080/01496399208018881

URL: http://dx.doi.org/10.1080/01496399208018881

SEPARATION SCIENCE AND TECHNOLOGY, 27(3), pp. 295–311, 1992

A Theoretical Model for the Separation of Glucose and Fructose Mixtures by Using a Semicontinuous Chromatographic Refiner

---

KWANG NAM LEE and WON KOOK LEE*
DEPARTMENT OF CHEMICAL ENGINEERING
KOREA ADVANCE INSTITUTE OF SCIENCE AND TECHNOLOGY
P.O. BOX 150, CHEONGRYANG, SEOUL, SOUTH KOREA

Abstract

The separation of a glucose and fructose mixture was experimentally performed by using a semicontinuous chromatographic refiner (SCCR) packed with Ca^{2+} ion in the form of DOWEX 50W 12X resin. The plug flow model with velocity-dependent mass transfer resistance was presented for calculating both products and on-concentrations in the SCCR unit, and the validity of the model was experimentally confirmed.

INTRODUCTION

The superiority of chromatography for separating complex mixtures as compared to conventional separation methods has been demonstrated (*1*). However, chromatographic separation normally operates in a batchwise manner, so complete separation or total resolution has to be performed if pure products are required. Thus, a recycle is usually necessary and the throughput is very low. The possibility of overcoming this disadvantage by operating the chromatographic equipment in a continuous countercurrent mode has been investigated (*2*). But many problems associated with the circulation of a solid adsorbent have occurred, so that alternative processes in which an effective countercurrent flow of the adsorbent can be achieved by moving the feed and having draw-off points at intervals through a fixed adsorbent bed have been developed. The alternative processes which have been the most successful can be divided into two types. One is the SORBEX type, developed by UOP (*3*), and the other is the semicontinuous chromatographic refiner (SCCR), developed by Barker et al. (*4*). A useful and

---

*To whom correspondence should be addressed.

comprehensive review of these two types has been given by Ruthven et al. (*5*). In an SCCR unit, a mathematical model which can predict both products and on-concentrations is needed to avoid dilution of the products. However, little study has been done on the model equation of the SCCR unit. In many articles (*6–8*) the equilibrium stage concept was used, and Ching et al. (*9*) used the steady-state axial dispersed plug flow model in terms of an equivalent countercurrent system to predict the performance of the SCCR unit. But when HETP is velocity-dependent, as in this work, the plate concept is not appropriate because the SCCR unit has three different flow rate zone (e.g., prefeed, postfeed, and purge sections). Also, the steady-state model cannot predict the product profiles with time. In this work an experimental and theoretical study of the performance of the SCCR unit for the separation of glucose and fructose is reported.

OPERATION PRINCIPLE OF THE SCCR UNIT

The countercurrent movement is simulated by sequencing a system of inlet and outlet port functions around 12 stainless steel columns. Each of these columns was packed with a calcium-charged DOWEX 50W 12X resin. Figure 1 illustrates the operation principle of the SCCR unit in the separation of a glucose and fructose mixture. In (A) the feed enters Column 7. The less strongly adsorbed glucose moves with the eluent (distilled water), which enters the system at Column 2 and exits with glucose from Column 12. The fructose, the strongly adsorbed component due to the formation of a chemical complex with Ca^{2+}, is preferentially retained by the resin. After a switch time, the position of the inlet and outlet port is advanced by one column (B). This simulation has the same effect as the movement of fructose with the stationary phase. At the end of 12 such switches, when each column has served as a purge entry, eluent entry, glucose exit, and feed column, a cycle is completed. After a number of cycles a pseudoequilibrium state is reached as the shapes of the glucose and fructose profiles become uniform and reproducible from cycle to cycle.

DESCRIPTION OF THE EQUIPMENT

The equipment was made up of twelve 1-cm-diameter stainless steel columns with packed lengths of 30 cm linked alternately top and bottom to form a closed loop. Three specially designed distributors which each have one inlet and 12 outlets were used to control purge, eluent, and feed inlet. Two three-way valves and one on–off valve were located on each column (Fig. 2). One three-way valve was for eluent or purge inlet from each distributor, and the other was for glucose-rich and fructose-rich products and the transfer line to the next column. One on–off valve was used

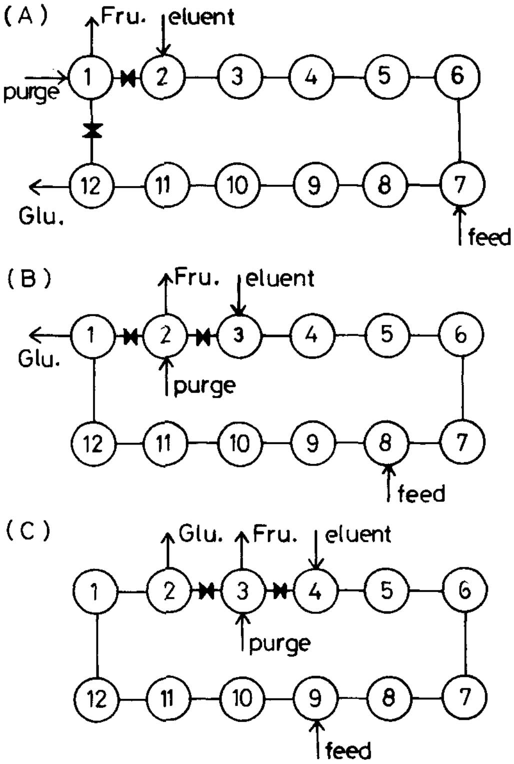

FIG. 1. Operation principle of the SCCR unit.

only as the feed inlet from the distributor. All columns were surrounded by a constant temperature enclosure.

CHROMATOGRAPHIC MEASUREMENTS

In order to characterize the equilibrium and kinetic properties of the adsorbent, a series of chromatographic measurements was carried out at 50°C on 12 of the columns. Using the dispersed plug flow model and Gluekauf's linear driving force approximation, the means and variances of the response peaks were calculated according to the usual expression.

$$\bar{t} = \int_0^\infty ct\,dt \Big/ \int_0^\infty c\,dt \tag{1}$$

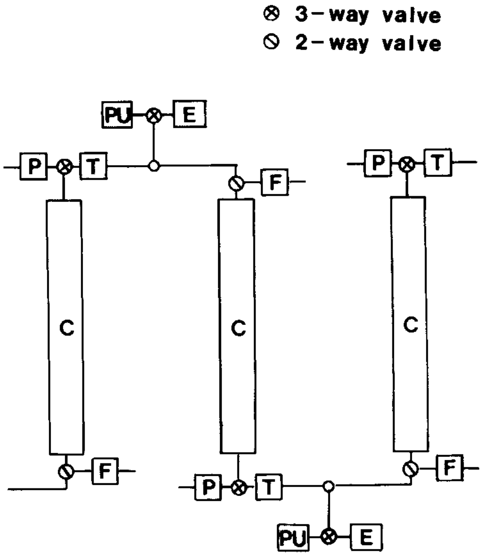

FIG. 2. Schematic arrangement of columns and valves. C, column; PU, purge line; E, eluent line; P, product line; F, feed line; T, transfer line

$$\sigma^2 = \int_0^\infty c\,(t - \bar{t})^2\,dt \Bigg/ \int_0^\infty c\,dt \tag{2}$$

For a linear system the mean retention time is related to the adsorption equilibrium constant by

$$\bar{t} = \frac{L}{v}\left(1 + \frac{1 - \epsilon}{\epsilon} K\right) \tag{3}$$

The chromatographic HETP is given by

$$\begin{aligned} H &= \frac{\sigma^2}{\bar{t}^2} L \\ &= 2\frac{D_L}{v} + 2v\left(\frac{1 - \epsilon}{\epsilon}\right)\frac{1}{K}\frac{1}{k}\left(1 + \frac{\epsilon}{(1 - \epsilon)K}\right)^{-2} \end{aligned} \tag{4}$$

where k is the effective overall mass transfer coefficient, defined by

$$\partial q/\partial t = k(q^* - q) = k(Kc - q) \tag{5}$$

Blue dextran, which because of its size (molecular weight = 2,000,000) does not penetrate the resin, was used as a tracer to estimate the void fraction, ϵ, and the value obtained from its mean retention time was 0.372. Values of $\bar{t}$ for both glucose and fructose are plotted against (L/v) and shown in Fig. 3. The equilibrium constants for glucose and fructose ($K_G = 0.123$, $K_F = 0.310$) are obtained from the slopes. The axial dispersion in a liquid system is proportional to the flow rate (*10*):

$$D_L = \eta v d \tag{6}$$

Thus the value D_L/v may be constant and can be calculated from the intercept of HETP vs v. The effective overall mass transfer coefficients can be calculated from the same plot with known values of the equilibrium constants. But if the axial dispersion effect is negligible, the effective overall mass transfer coefficient can be described by the velocity dependence:

$$k(v) = \frac{av}{v + b} \tag{7}$$

The above two models are compared in Table 1 and Fig. 4 with the experimental results. There is no difference between the two models. This

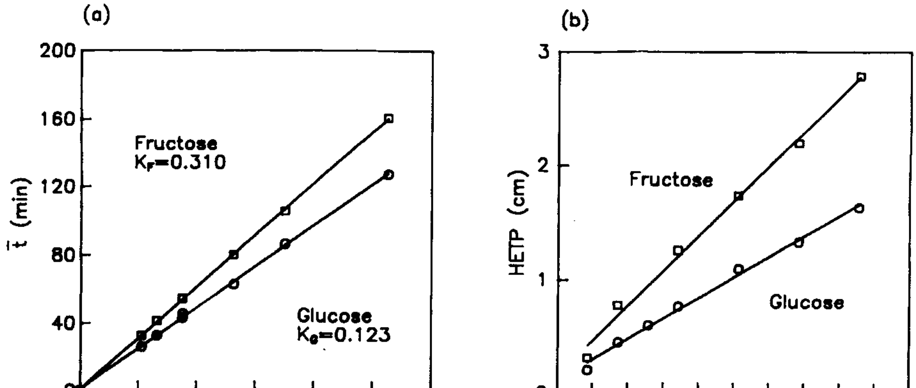

FIG. 3. (a) Mean retention time plotted against L/v. (b) HETP as a function of fluid velocity.

TABLE 1
Comparison of Two Models

	Axial dispersed plug flow model with constant mass transfer resistance		Plug flow model with velocity-dependent mass transfer resistance	
	Glucose	Fructose	Glucose	Fructose
Axial dispersion coefficient (cm^2/min)	$0.057v$	$0.077v$	—	—
Effective overall mass transfer coefficient (min^{-1})	3.155	2.941	$\frac{3.155v}{v + 1.315}$	$\frac{2.941v}{v + 1}$

is because the axial dispersion effect is lumped to the velocity-dependent overall mass transfer resistance.

MATHEMATICAL TREATMENT OF THE SCCR UNIT

In the SCCR unit, each adsorption column can be considered to be a fixed bed except at the moment of moving purge, eluent, and feed column. Because the plug flow model with a velocity-dependent overall mass transfer resistance satisfactorily describes the chromatographic responses, mass balance equations with respect to the concentrations of the mobile phase c and the stationary phase q and boundary condition at the column exit

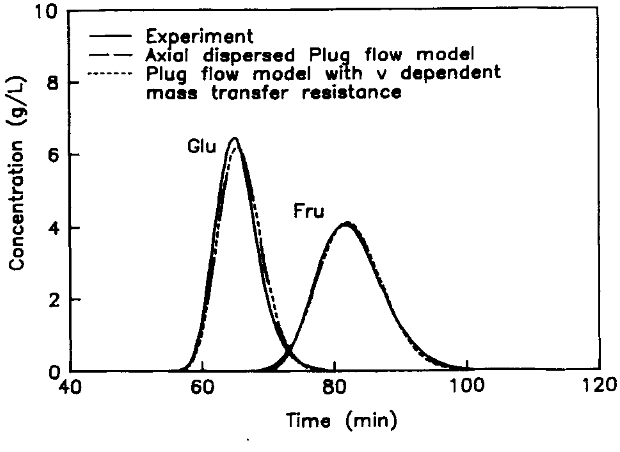

FIG. 4. Comparison of experimental and theoretical curves of two models when the volumetric flow rate is 2 cm^3/min.

can be given by Eqs. (8)–(10), which are set positive for the direction of liquid flow:

$$\frac{\partial c_i}{\partial t} = -v_i \frac{\partial c_i}{\partial z} - \frac{1 - \epsilon}{\epsilon} k(v_i)(Kc_i - q_i) \tag{8}$$

$$\partial q_i / \partial t = k(v_i)(Kc_i - q_i) \tag{9}$$

$$\partial c_i / \partial z = 0, \qquad \text{at } z = L \tag{10}$$

where the subscript i refers to the column number (1 to 12).

The following conditions are written for the inlet points between columns when the feed enters Column 7: At the inlet point of the purge stream:

$$c_{1,0} = 0.0 \tag{11}$$

At the inlet point of the eluent stream:

$$c_{2,0} = 0.0 \tag{12}$$

At the inlet points between columns:

$$c_{i,0} = c_{i-1,1} \ (i = 3, \ldots, 6, 8, \ldots, 12) \tag{13}$$

At the inlet point of the feed stream:

$$c_{7,0} = \frac{v_6 c_{6,1} + v_f c_f}{v_7} \tag{14}$$

where the first subscript is the column number and second subscript denotes the inlet (0) and outlet (1) of the liquid stream in each column.

Under the assumption that the components do not interact in the linear isotherm, the numerical solution of the transient model of each fixed bed was performed through the orthogonal collocation method (*11*) that reduces the original system to a system of ordinary differential equations. This system was solved through a fourth-order Runge–Kutta method. Selection of seven collocation points at each fixed bed gave sufficient precision to calculate the theoretical profiles under the experimental conditions of this work. When the columns are advanced at the end of a switch time, the concentrations corresponding to collocation points are also rearranged in the direction of the arrows illustrated in Fig. 5 according to column

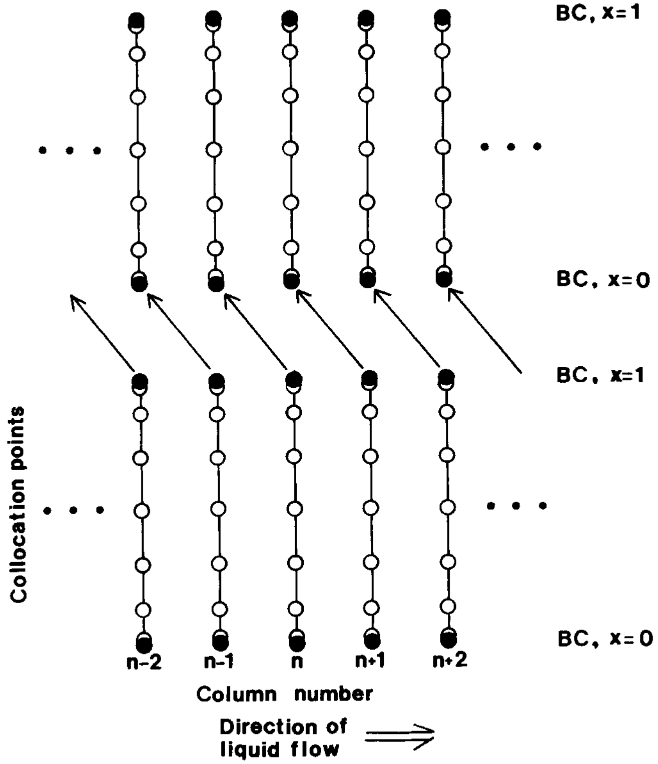

FIG. 5. Schematic explanation of calculation method in the SCCR unit using orthogonal collocation method.

movement. With this integration method, the pseudoequilibrium concentration profile can be calculated.

EXPERIMENTAL

The feed solution used in the SCCR unit contained 10 g/L each of glucose and fructose dissolved in distilled water. Liquid samples were taken from the exit of each column and analyzed by HPLC (Waters Co.) by using an "Aminex 87C" column (Bio-Rad Co.). The stainless steel analytical column was 4 mm in diameter and 250 mm in length. The packing consisted of 9 μm sulfonated divinyl benzene–styrene beads in the Ca^{2+} form. Elution was performed at 85°C at a fluid (distilled water) velocity of 0.4 cm^3/min. Under these conditions the retention times for the glucose and fructose peaks are 4.3 and 5.5 min, respectively. All runs in the SCCR unit were carried out at 50°C. Samples were taken as close as possible to the end of the switch interval for on-concentrations and split into 10 parts in the given switch time for the glucose- and fructose-rich products.

RESULT AND DISCUSSION

In describing the operating principles of the SCCR unit it was noted that the packing of the column is moved countercurrent to the direction of mobile phase flow at a correct rate; that is, the slow-moving component can be made to travel with the packing and the fast-moving component with the mobile phase. Thus, the required flow conditions may be conveniently specified in terms of the dimensionless parameter γ [$= (1 - \epsilon) Ku/\epsilon v$], which is the ratio of the downward flow in the adsorbed phase to the upward flow in the mobile phase.

$$\text{prefeed section: } \gamma_G < 1.0,\ \gamma_F > 1.0$$

$$\text{postfeed section: } \gamma_G < 1.0,\ \gamma_F > 1.0 \tag{15}$$

As applied to the SORBEX type by Ching et al. (*12*), these inequalities can be similarly translated into two equations relating the flow rate ratios E/S and F/S and the parameter α (>1.0) by which the inequalities are satisfied.

$$\text{prefeed section: } E/S = K_G\alpha$$

$$\text{postfeed section: } E/S + F/S = K_F/\alpha \tag{16}$$

For each section of the SCCR unit, two equations of type (16) relating four variables E, S, F, and α are given. Thus, by specifying two variables, the other two variables can be obtained. Here we simply specify the switch time, which determines the variable S, and the parameter α is fixed to a 10% margin to define the eluent and the feed flow rate.

In the purge section, excess flow is needed only to wash out the tracer within a switch time:

$$\text{purge section: } \gamma_F < 1.0 \tag{17}$$

Sometimes this excess flow may cause dilution of the product, so that some trials are needed to determine the proper purge rate.

Because each column contains the eluent phase in the void volume, this amount has to be compensated for in the eluent rate to get the actual eluent rate in an SCCR unit:

$$E^{\cdot} = E + A\epsilon u \tag{18}$$

Steady-state concentration profiles were measured under the six sets of operating conditions summarized in Table 2, and the required flow rates were obtained with Eqs. (16) and (18). Representative profiles are shown in Fig. 6 together with the theoretical profiles calculated from the rate model. Theoretical curves provide a reasonably good representation of the experimental profiles. Although flow conditions of Run 2 differ from those of Run 4, similar profiles can be obtained with the same flow ratios (γ values). The small difference in the theoretical profiles seems to be due to the velocity-dependent kinetic parameter.

The feed flow rate was increased in Run 5 to the range where the inequality constraints were satisfied (Fig. 7). Although the glucose profiles were not changed, the fructose profiles were improved some compared with Run 2. Thus, in the fructose-rich product, the output concentration and its recovery could be improved. However, the trailing edge of the fructose profile did not drop sharply to zero, so some impurity in the glucose-rich product was obtained. By increasing the feed flow rate, the product concentration of the fructose-rich product is increased but at the expense of product purity of the glucose-rich product.

It is of interest to investigate the number of total columns used in the SCCR unit with regard to the complexity of the operation and the cost of the equipment. In Run 6, a total of six columns, each 60 cm long, was used in operating the SCCR unit, and the eluent and feed rates were the same as in Run 2 but the switch time and purge rate were not (Fig. 8). Although there was some impurity in both products, it was possible to operate with six columns and obtaining a high-fructose syrup with 55 to 90% fructose. Further calculation showed that SCCR operation with eight columns, each 45 cm long, could lead to a theoretical purity of 99.9% for both products. Thus, there is no need to operate with twelve columns.

Various purge rates were tested while maintaining the other flow rates constant (Runs 1, 2, and 3). Because the fructose- and gluocse-rich products can be accurately estimated if the collection times of the products are properly selected, substantial dilution of the product can be avoided. At this point the "critical" dilution was arbirarily defined as that value where the product concentration was about 10% of the feed concentration. In all experiments, the fructose-rich products higher than the "critical" dilution were collected and the glucose-rich products were collected as soon as the glucose started to exit. The experimental results of these techniques are

TABLE 2
Experimental Conditions in the Operation of the SCCR

Run no.	Switch time (min)	Eluent rate (cm³/min)[a]	Feed rate (cm³/min)	Purge rate (cm³/min)	γ_G		γ_F		Purge section
					Prefeed	Postfeed	Prefeed	Postfeed	
1	3	0.67 (3.59)	0.72	7.0	0.91	0.44	2.28	1.10	0.22
2	3	0.67 (3.59)	0.72	5.0	0.91	0.44	2.28	1.10	0.31
3	3	0.67 (3.59)	0.72	3.0	0.91	0.44	2.28	1.10	0.51
4	4	0.50 (2.69)	0.54	5.0	0.91	0.44	2.29	1.10	0.23
5	3	0.67 (3.59)	0.83	5.0	0.91	0.40	2.28	1.02	0.31
6	6	0.67 (3.59)	0.72	2.5	0.91	0.44	2.28	1.10	0.61

[a] Values in parentheses are the actual flow rates.

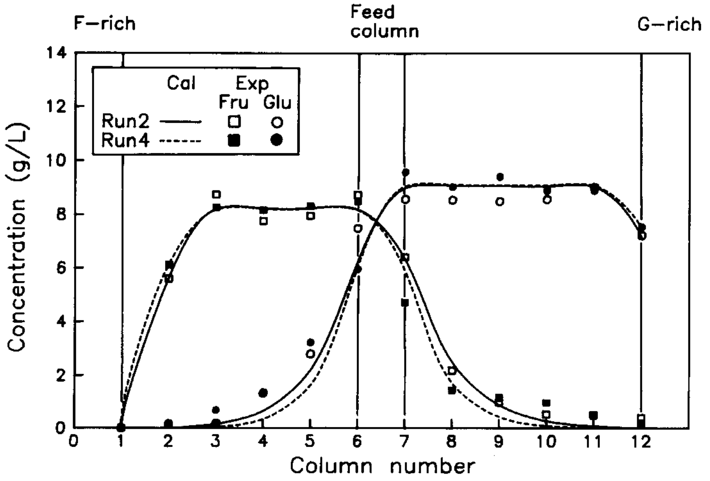

FIG. 6. Experimental and theoretical concentration profiles of Runs 2 and 4.

summarized in Tables 3 and 4, respectively. In Runs 3 and 6, the purge rates, 3 and 2.5 cm^3/min, were not enough to strip the fructose within a switch time (see Figs. 9 and 10). But in all experiments, because the fructose below the "critical" dilution was discarded and the glucose was collected when it started to exit, the purge rates listed above could be successfully

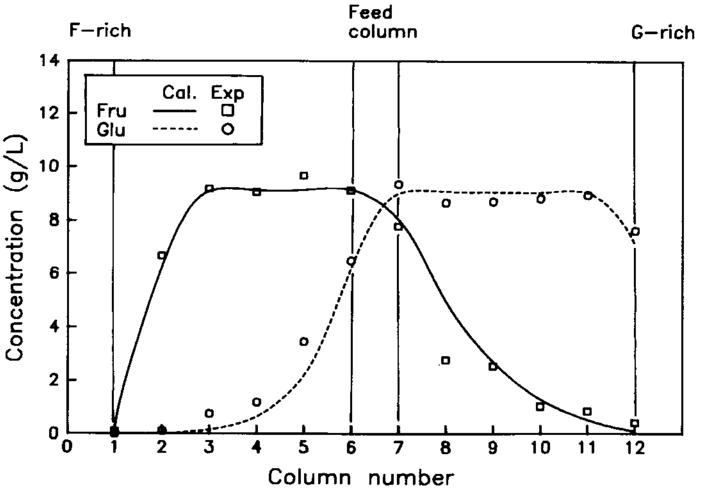

FIG. 7. Experimental and theoretical concentration profiles of Run 5.

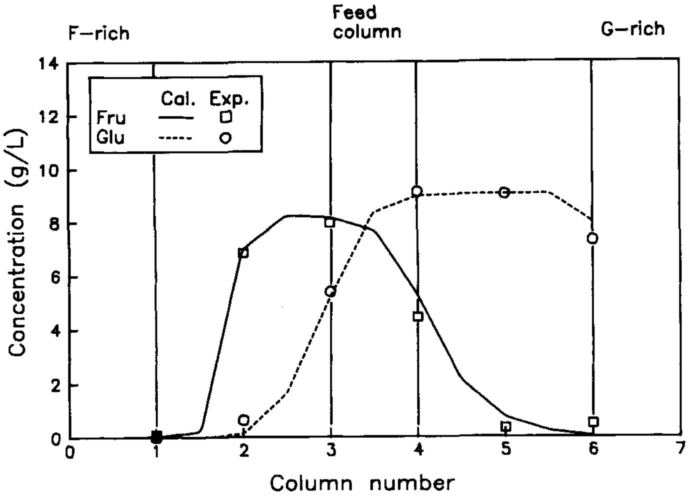

FIG. 8. Experiment and theoretical concentration profiles of Run 6.

used to strip the fructose and maintain the purity. Therefore, such purge rates can decrease the eluent requirement and the discarded dilutions can be recycled as eluents to recover all the sugar feeding to the SCCR unit.

CONCLUSION

The separation of a glucose and fructose mixture by the use of a semicontinuous chromatographic refiner was performed experimentally. In an SCCR unit, by considering each adsorption column to be a fixed bed except at the moment of moving purge, eluent, and feed columns, the concentration profiles could be represented by the plug flow model with an overall effective rate coefficient, including the effect of axial dispersion. The numerical values could be calculated by the orthogonal collocation method which can simulate the column switching by rearranging the concentrations coresponding to the collocation points backward, by one column, at the end of a switch time. The glucose- and fructose-rich product profiles were accurately predicted by this calculation method, so both products could be obtained more efficiently.

SYMBOLS

A	cross-sectional area of column (cm^2)
a, b	defined in Eq. (7)
c	fluid phase concentration of sorbate (g/L)
c_f	feed concentraton (g/L)

TABLE 3
Experimental Results in the Fructose-Rich Product[a]

Run no.	Switch time (min)	Purge rate (cm^3/min)	Product collection time (min)	Average concentration (g/L)	Purity (%)	Recovery (%)
1	3	7.0	0 to 0.9	2.69 (2.79)	94.1 (99.9)	78.3 (81.3)
2	3	5.0	0 to 1.2	2.91 (2.94)	96.8 (99.9)	80.7 (81.7)
3	3	3.0	0 to 2.1	3.16 (2.94)	93.0 (99.9)	92.1 (85.8)
4	4	5.0	0 to 1.6	3.28 (3.06)	93.0 (100)	91.1 (85.0)
5	3	5.0	0 to 1.2	3.34 (3.25)	96.4 (99.9)	94.4 (99.0)
6	6	2.5	0 to 4.2	3.60 (3.72)	91.0 (98.9)	87.6 (90.5)

[a] Values in parentheses are the theoretical results.

TABLE 4
Experimental Results in the Glucose-Rich Product[a]

Run no.	Switch time (min)	Raffinate rate (cm^3/min)	Product collection time (min)	Average concentration (g/L)	Purity (%)	Recovery (%)
2	3.0	1.39 4.31*	1.8 to 3.0	3.79 (4.20)	94.9 (100)	97.5 (99.3)
4	4.0	1.04 3.23*	2.4 to 4.0	4.14 (4.26)	95.9 (100)	95.9 (99.1)
5	3.0	1.50 4.42*	1.8 to 3.0	4.43 (4.65)	93.6 (99.2)	94.4 (99.0)
6	6.0	1.39 4.31*	3.6 to 6.0	3.79 (4.20)	93.8 (99.7)	90.6 (99.5)

[a] Values in parentheses are the theoretical results. Asterisks indicate the actual flow rates in the postfeed section.

D_L	axial dispersion coefficient (cm^2/min)
E	eluent flow rate (cm^3/min)
E^*	actual eluent flow rate in the SCCR unit (cm^3/min)
F	feed flow rate (cm^3/min)
K	adsorption equilibrium constant ($= q^*/c$)
k	effective overall mass transfer coefficient (min^{-1})
L	length of adsorbed bed
q	sorbate concentration in adsorbed phase (g/L)

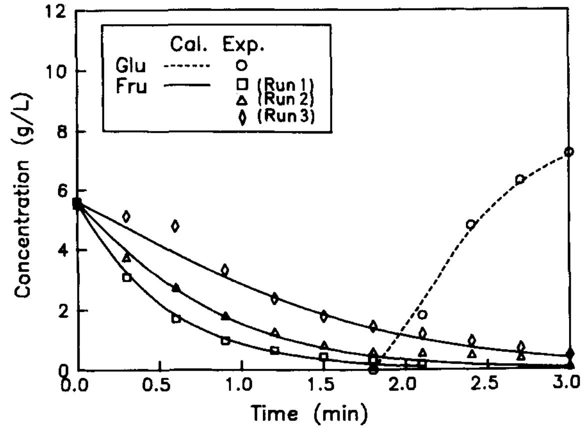

FIG. 9. Experimental and theoretical concentration profiles of glucose- and fructose-rich product (Runs 1, 2, and 3).

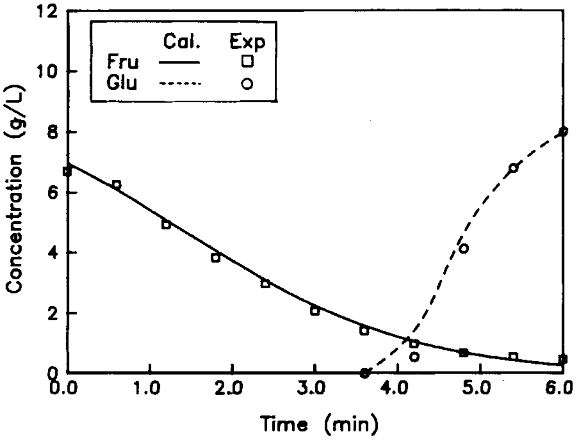

FIG. 10. Experimental and theoretical concentration profiles of glucose- and fructose-rich product (Run 6).

S	hypothetical adsorbent recirculation rate in equivalent countercurrent system (cm^3/min)
SCCR	semicontinuous chromatographic refiner
t	time (min)
$\bar{t}$	mean retention time (min)
u	hypothetical solid velocity ($= L/\tau$) (cm/min)
v	interstitial fluid phase velocity (cm/min)
v_f	feed flow rate (cm/min)
x	dimensionless axial distance ($= z/L$)
z	axial distance in adsorbent bed (cm)
α	margin defined in Eq. (16)
γ	dimensionless parameter [$= (1 - \epsilon)Ku/\epsilon v$]
ϵ	void fraction
η	scale of axial eddy dispersion
τ	switch time
σ	standard deviation of response peak (min)

Subscripts

F	fructose
G	glucose

REFERENCES

1. M. V. Sussman, *Chem. Tech.*, *11*, 260 (1976).
2. P. E. Barker and D. Critcher, *Chem. Eng. Sci.*, *13*, 82 (1960).
3. D. B. Broughton, *Chem. Eng. Prog.*, *64*(8), 60 (1968).

4. P. E. Barker and R. E. Deeble, *Anal. Chem.*, *45,* 1121 (1973).
5. M. R. Ruthven and C. B. Ching, *Chem. Eng. Sci.*, *44*(5), 1011 (1989).
6. C. B. Ching, *J. Chem. Eng. Jpn.*, *16*(1), 49 (1983).
7. P. E. Barker and G. Ganetsos, *Sep. Sci. Technol.*, *22,* 2011 (1987).
8. P. E. Barker and S. Thawait, *Chem. Ind.*, *7,* 817 (1983).
9. C. B. Ching and D. M. Ruthven, *Chem. Eng. Sci.*, *40*(6), 877 (1985).
10. D. M. Ruthven, *Principle of Adsorption and Adsorption Process,* Wiley, New York, 1984.
11. J. Villadsen and M. L. Michelson, *Solution of Differential Equation Models by Polynomial Approximation,* Prentice-Hall, Englewood Cliffs, New Jersey, 1978.
12. C. B. Ching, D. M. Ruthven, and K. Hidajat, *Chem. Eng. Sci.*, *40*(8), 1411 (1985).

Received by editor February 22, 1991